JOURNAL OF MATERIALS SCIENCE 18 (1983) 64–80

Structure and oxygen-barrier properties of metallized polymer film

E. H. H. JAMIESON, A. H. WINDLE
Department of Metallurgy and Materials Science, University of Cambridge, Pembroke Street, Cambridge, UK

The structure of thin (10 to 50 nm) aluminium layers vacuum deposited on to polyester film is examined using both transmission electron microscopy and light microscopy. The density of pinhole defects in the aluminium coating, quantified by an image analysing microscope, is shown to determine the permeability of the film to oxygen. Finite element calculations of the effect of various pinhole diameters and densities on the permeability agree with experiment, and also show that the barrier properties of the polymer layers immediately adjacent to the metal coating are critical in determining the deleterious effect of pinhole defects.

1. Introduction

The vapour deposition of materials, particularly metals, on to various substrates is exploited in a very wide range of technological situations. The literature on the topic is correspondingly extensive. This paper focuses on one particular aspect of the subject, that is, the structure and barrier properties of polymer film vacuum coated with a thin layer of metal.

Metallized polymer films are useful because they are decorative [1–4], because of their suitability for winding to form capacitors, and because their very good barrier properties commend them to packaging applications [5]. The market for metallized film is growing significantly, particularly in the packaging field where it is replacing aluminum foil which has a higher energy content. The majority of commercially metallized film consists of aluminium deposited on polyester, cellulose or even paper as the base. The aluminium coating is exceedingly thin (a few tens of nanometres is typical) so that for a 12 μm thick base film the ratio of coating thickness to film thickness approaches 1:1000. So, if one relates the polymer film thickness to the height of (say) a table, then the metal coating will be equivalent to the thickness of the tablecloth. This very thin coating has a profound influence not only on optical and electrical properties but also on the permeability of the film to gas. Polymers such as biaxially oriented polyester film, even though they are intrinsically good gas barriers, can have their barrier performance improved by a factor of several hundred by metallization.

The vast majority of structural studies of vacuum-deposited coatings have used inorganic substrates such as glass or halide crystals. Deposition of metals, at all but cryogenic temperatures, gives rise to a conventional crystalline structure. At early stages the metal forms small clusters or nuclei, a few nanometres in diameter which, as further metal vapour condenses grow and eventually coalesce. This form of growth is associated with the initial surface mobility of the freshly arrived atoms [6], and in addition there is evidence from electron microscopy, in an *in situ* deposition experiment, that the smaller nuclei are themselves mobile [7]. The coalescence of the nuclei to form a continuous film occurs at a thickness which depends on the mobility of the depositing atoms, the vacuum quality, and the rate of deposition, and can be observed by a sharp drop in film resistivity. In general the higher the rate of deposition the smaller the amount of metal at which coalescence is achieved [8]. There is evidence for substantial grain growth in the thin metal coating, and this process is seen as a mechanism for stress relief [9, 10].

0022–2461/83/010064–17$04.54/0 © *1983 Chapman and Hall Ltd.*

More recent work on thin aluminium films (up to 100 nm) deposited on to glass substrates confirms the importance of an oxide layer between the film and the substrate to ensure good adhesion [11]. Attention is drawn to a large compressive stress within the film possibly arising from the incorporation of oxygen during growth. An increase in adhesion with time is also noted. Blair and Ghate [12] have also confirmed earlier work regarding the effect of vacuum conditions on the thin film.

In this paper the structure of aluminium coatings deposited on to a polymer substrate is examined and various methods of measuring metal thickness compared. In qualitative terms the structure is not significantly different from that observed in metal layers deposited on to inorganic substrates. Particular attention, however, is paid to defects in the metal and these are related to the measured barrier performance of the coated film.

2. Experimental procedure

2.1. Vacuum metallization

The commercially metallized samples used in this work were supplied by a number of trade metallizers. The samples had all been produced in reel-to-reel machines, in which the polymer film is transversed at speeds of a few metres per second above aluminium held molten in resistance-heated boats made of boron nitride. A typical nominal vacuum for the process is 10^{-3} torr although it will be much higher in the region of the depositing metal because of the gettering action of the aluminium vapour. A commercial deposition rate will be around 500 nm sec^{-1}.

Laboratory metallized samples were produced individually in a small vacuum chamber. The aluminium was evaporated from a helical tungsten filament at a nominal vacuum of 10^{-5} torr. The deposition rate was controlled around 10 nm sec^{-1} by means of a quartz oscillator thickness gauge.

2.2. Thickness measurement

The thickness of the deposited aluminium layer was measured by four methods: X-ray fluorescence analysis calibrated by chemical analysis, multiple-beam interferometry [13], electrical resistivity, and X-ray diffraction line broadening. The resistivity measurements were modified from those often employed in quality control by eliminating the effect of contact resistance by measuring the resistance over two or more different lengths of metallized strip, and also be recalculating the resistivity of the aluminium to take account of the thinness of the film [14]. The X-ray line broadening made use of the Scherrer formula [15] which relates the film thickness to the half-width of the diffraction peak.

2.3. Measurement of permeability

The permeability of the metallized films to oxygen was measured using an Ox-Tran 100. In this equipment the transmitted oxygen is detected coulometrically for a preselected film temperature (20° C in this work). The system and sample is initially purged by an oxygen-free carrier gas, and the permeability only recorded once equilibrium conditions have been reached.

2.4. Microscopy

Transmission electron microscopy of the aluminum layer required its removal from the polymer film. This was achieved by first scoring the aluminum into 3 cm squares and then dissolving the polyethylene terephthalate by immersion in orthochlorophenol at 70° C for 3 h. The metal squares were washed several times in Analar ethanol and then placed on microscope grids as required.

The pinhole size distributions were measured with a light microscope and "Quantimet" image analysing computer.

3. Materials

Throughout the work, the system examined consisted of biaxially drawn polyester film vacuum-coated with aluminium. Coated film from industrial sources was compared with that metallized in the laboratory. The polyester used in the industrially prepared samples was, in general, 12 μm "Melinex" (ICI Ltd), while that used in the laboratory was exclusively so.

A range of grades of Melinex was examined. Fig. 1 shows the surface roughness associated with the filler particles added to "S" and 442 Melinex grades compared with the unfilled type "O" material. The surface roughness is derived from inhomogeneous deformation, associated with inbedded filler particles, which occurs during the biaxial drawing process. It improves handling by limiting adhesion (blocking) between adjacent layers. The three grades of Melinex are referred to below as polyesters: M"S", M"442" and M"O".

In the laboratory metallization the aluminium

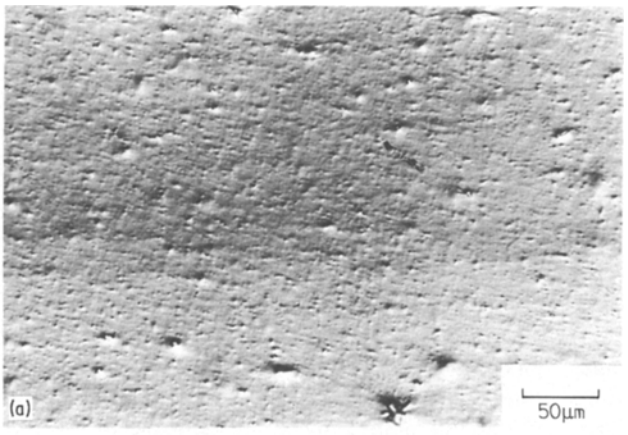

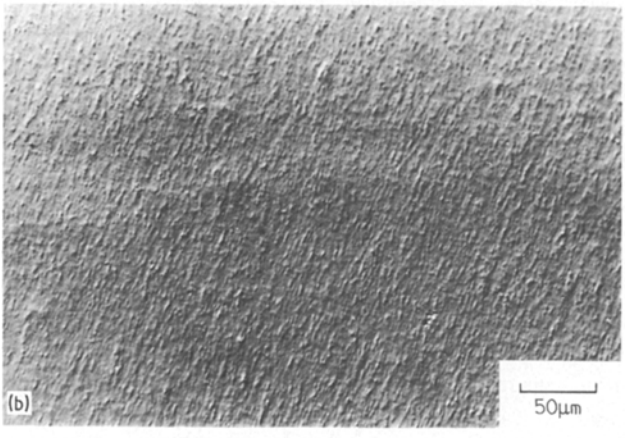

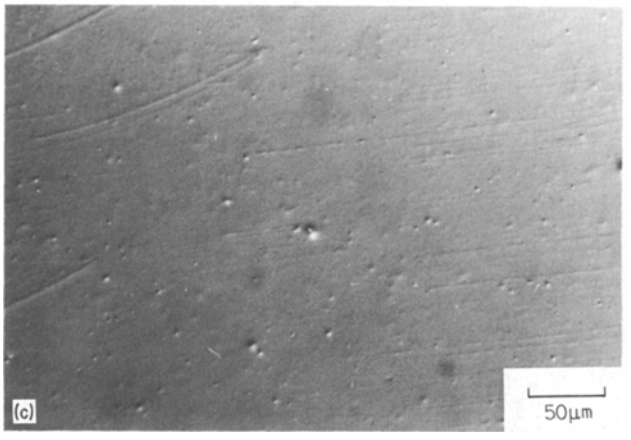

Figure 1 Surface topography of three grades of polyester film revealed using Normarski differential interference contrast (NDIC). The films are aluminium-coated to improve reflectance, but the metal layer plays no part in the structure seen at this magnification. (a) Melinex type S (M"S"). (b) Melinex type 442 (M"442"). (c) Melinex type O (M"O").

used was of 99.998% purity; in commercial reel-to-reel equipment, 99.95%.

4. Structure of the deposited aluminium layer

The thickness of the deposited aluminium ranged from 10 to 70 nm. The thickness was measured by a variety of techniques which produced broadly comparable results. Measurements made on the same sample of film using the different techniques are summarized in Table I. In general, the methods of multiple-beam interferometry and X-ray fluorescence include the thickness of the oxide layers on the metal and give values around 10 nm greater than X-ray line broadening and resistivity. Such a result would be consistent with a 5 nm thick oxide layer which is not unreasonable. The aluminium layer showed marked preferred orientation, with

TABLE I Thickness of aluminium deposit on two films measured using different techniques

Method	Measured thickness (nm)	
	Sample 1	Sample 2
Resistivity	33	20
X-ray line broadening	33	26
Interferometry	41	34
X-ray fluorescence	47	35

[111] aligning normal to the plane of the film. The texture was developed to the extent that the 200 reflection from the surface plane was completely suppressed. Fig. 2 is a transmission electron micrograph of the deposited metal as stripped from the polymer film. The grain size was observed to be the same order as the layer thickness, in accord with previous studies on aluminium on glass [11]. It is about 70 nm in this sample. The grain size was also dependent on the vacuum maintained during deposition; 8×10^{-5} torr gave a grain size of 36 nm while a better vacuum of 2.8×10^{-5} torr produced grains of 63 nm for the same layer thickness deposited at the same rate. Presumably this points to the role played by incorporated impurities in pinning grain boundaries and thus inhibiting grain growth. Overall, the structure of the aluminium layer deposited on to the polyester film, whether by laboratory (batch) or commercial (continuous) metallization, was similar to that reported for a wide range of systems involving aluminium on inorganic substrates [6, 12].

5. Pinhole defects

An important objective of commercial metallization is the improvement of the barrier properties of the polymer film, and the integrity of the aluminium layer is thus of considerable significance. Examination of metallized film in transmitted light invariably reveals pinhole-type defects in the metal layer which are not associated with corresponding defects in the polymer substrate. Fig. 3a shows a typical distribution of pinholes in a commercially metallized specimen. The density here (number per unit area) is around 25 mm^{-2} which is comparatively low. Fig. 3b shows the same sample at higher magnification in which a background of very faint and presumably very small pinholes is also visible. Pinholes ranging from 1 to 10 μm and above were observed in the transmission electron microscope. It is significant that none smaller than 1 μm was seen. Fig. 4 shows an example of a pinhole 3 μm across, which is not obviously the result of mechanical damage although there is evidence for a small amount of rumpling around the edges. Such features are typical of all isolated pinholes. In contrast, some commerically produced films show distinct defect arrays which are made up of runs of pinholes (Fig. 5). Examination of the runs in the electron microscope shows features which suggest mechanical damage, possibly the result of a hard particle being drawn across the surface. Fig. 6 illustrates this. The displaced aluminium is folded up at the head of each hole and there is some intergranular cracking. It is possible that the distinctive "ticks" and "V"s are produced when slipping occurs as a result of spontaneous readjustments in the tension of the film on the reel. Fig. 7 shows a damage run examined first in transmitted light a, and then in the transmission electron microscope b. A small

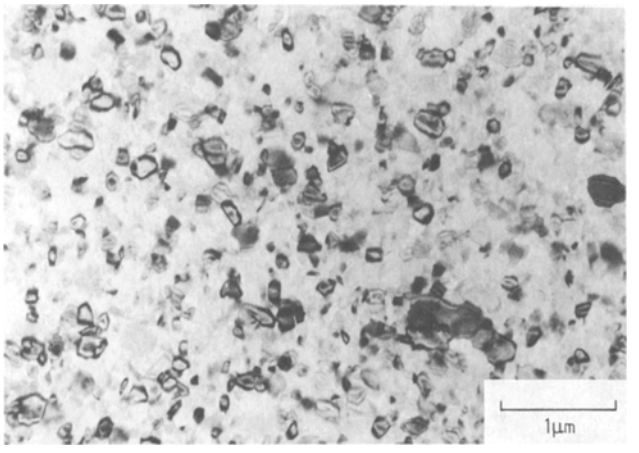

Figure 2 Transmission electron micrograph of aluminium layer vacuum deposited on to Melinex "O". The polymer was dissolved away prior to examination.

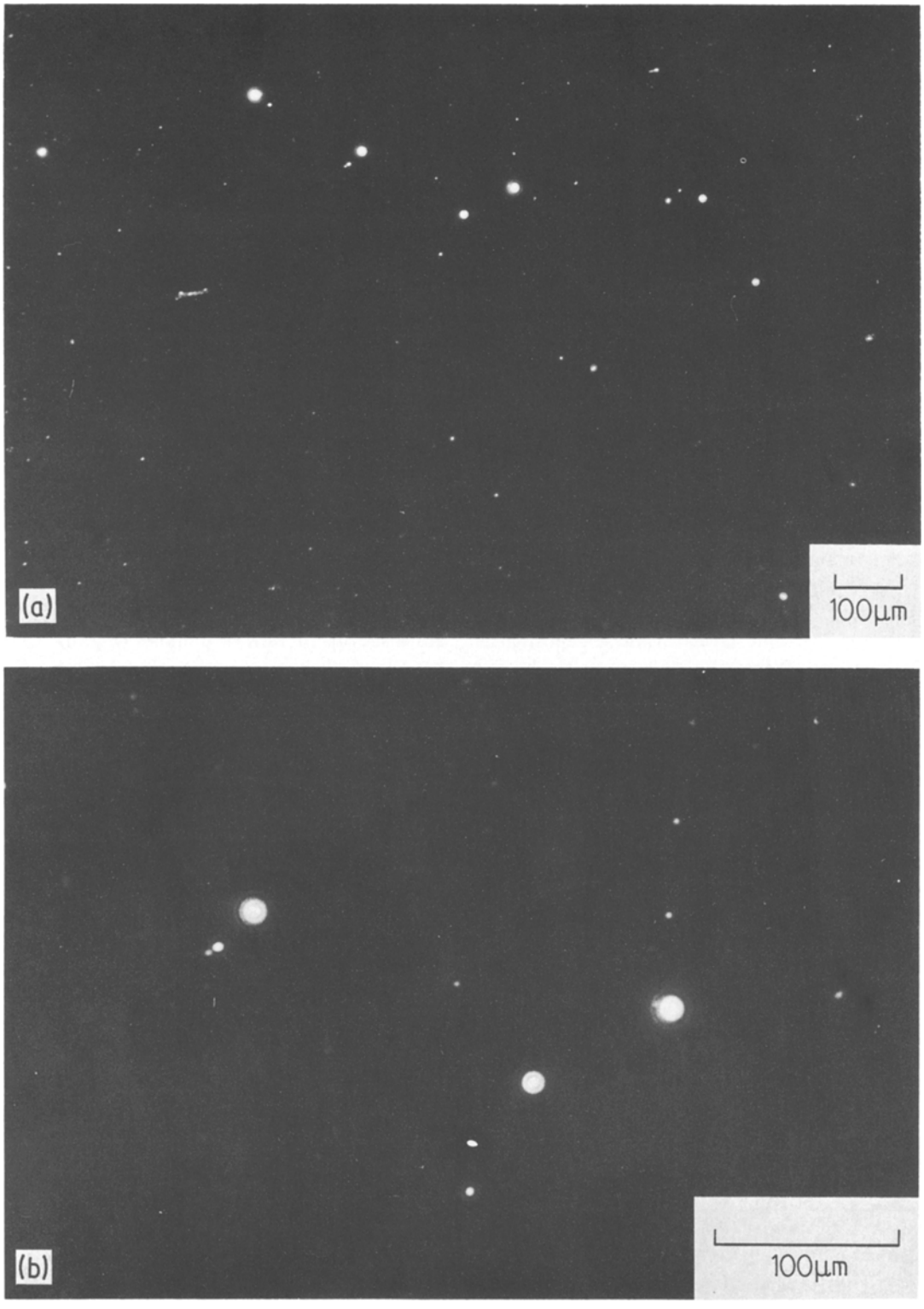

Figure 3 Transmission light micrographs of metallized (M"S") film showing pinhole defects.

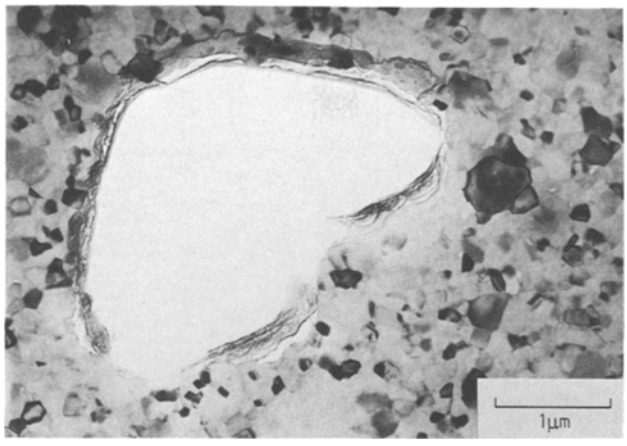

Figure 4 Transmission electron micrograph of a pinhole approximately 3 μm diameter seen in the stripped aluminium layer.

particle, possibly responsible for the damage, may be seen at the left extremity of the run in Fig. 7b. Occasionally, films in which the metal deposit had been subsequently lacquered by a wet process showed inordinately high levels of damage (Fig. 8). This may in some way be associated with poor setting of the doctor blade which removes excess lacquer during the process.

6. Origin of pinhole defects

In order to indentify the cause of pinholes in the commercially produced material, a series of equivalent films was metallized in a small laboratory evaporator.

If such films were handled carefully, then they appeared to be free from pinholes in the 1 to 10 μm range, although larger defects of 25 to

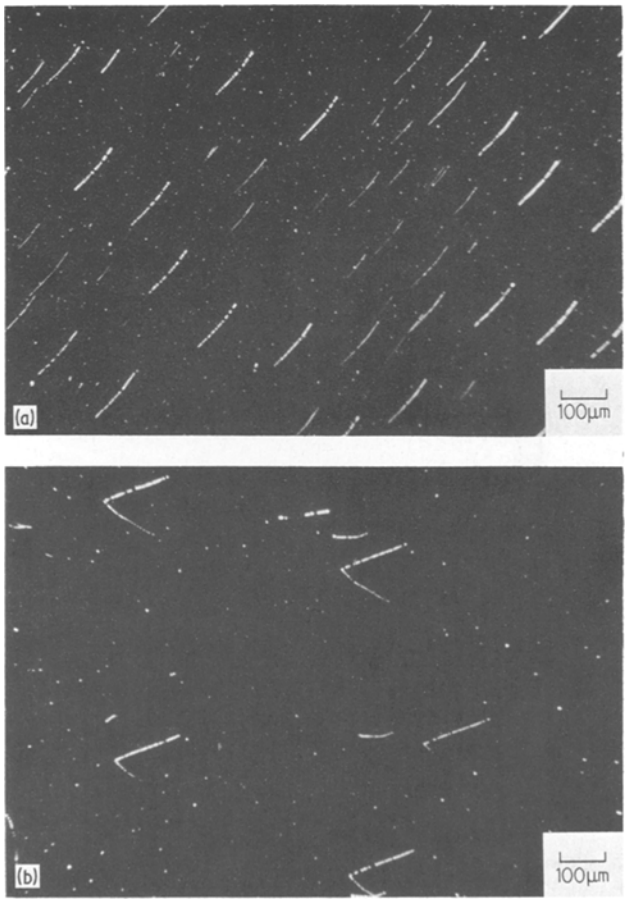

Figure 5 Transmission light micrographs showing (a) runs and (b) "V"s of pinholes in commercially reeled film.

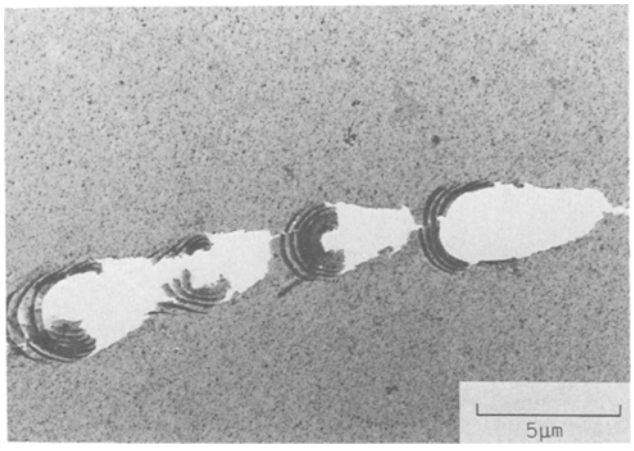

Figure 6 Transmission electron micrographs of a run of pinholes which appears to be the result of scuffing damage.

50 μm, obviously associated with dust particles, were sometimes apparent. If, however, the metal surface was lightly rubbed with a camel-hair brush, then 1 to 10 μm pinholes were seen to develop. After two or three passes with the brush development was complete, and subsequent prolonged treatment (in excess of 100 passes) produced no further pinholes. This indicates that the pinholes are related to specific weak-points in the metal layer and not the consequence of straightforward mechanical damage as indeed can be produced by much more severe abrasion. Fig. 9 shows the laboratory metallized film before and after treatment with the camel hair brush. In Fig. 9a particles are seen as dark specks, the film having been fairly lightly metallized to ensure some general transparency to light. The positions of many of these particles correlate perfectly with the positions of developed pinholes in Fig. 9b. This experimental approach has also been used in the investigation of defects in unbacked metal filters [16]. Fig. 10 shows the results of a "Quantimet" analysis of pinhole-size distribution which compare the as-metallized (Fig. 10a) and developed (Fig. 10b) laboratory samples with the commercially produced material (Fig. 10c). The only pinholes visible in the unhandled film are large ones result-

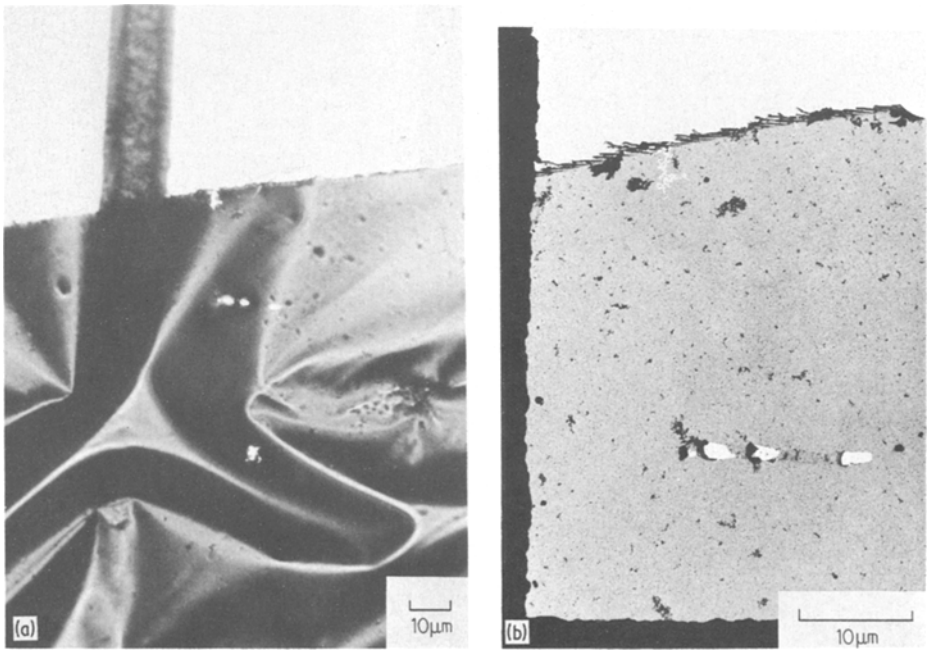

Figure 7 A run of pinholes in a stripped aluminium layer, photographed (a) in transmitted light, (b) in the TEM. The particle which caused the damage is possibly visible at the left extremity of the "run".

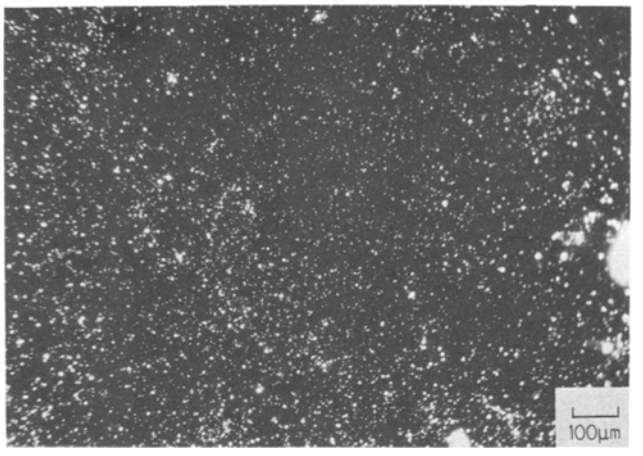

Figure 8 Severe pinhole damage sometimes seen in commercially produced samples in which a protective coat of lacquer has substantially been laid down on the aluminium film.

ing from the presence of laboratory dust, hairs, etc., on the film surface. Similar large pinholes are not seen in films produced commercially. Light brushing of the laboratory-produced films develops a pinhole distribution (Fig. 10b) which peaks between 1 and 2 μm and is similar to that apparent in commercial material (Fig. 10c). It seems then, that the pinholes are closely associated with the presence of particles on the film surface during metallization. It is probable that they are shadows behind dust particles which are present on the surface of the polymer during metallization, the shadows being revealed if the particles are subsequently dislodged. The shadowing effect of the surface particles is readily apparent, if the metal is deposited at an oblique angle to the surface (Fig. 11).

It is not immediately clear whether the surface particles are laid down in the early stages of the metallization process or whether they are already present on the surface of the polymer film. However, examination of polyester film on unreeling and prior to metallization, revealed a distribution of surface particles which could account for subsequent pinhole formation. Analysis of the size distribution of the dust in Fig. 12a also correlates well with that typical of pinholes (Fig. 12b).

A large number of surface particles on polyester

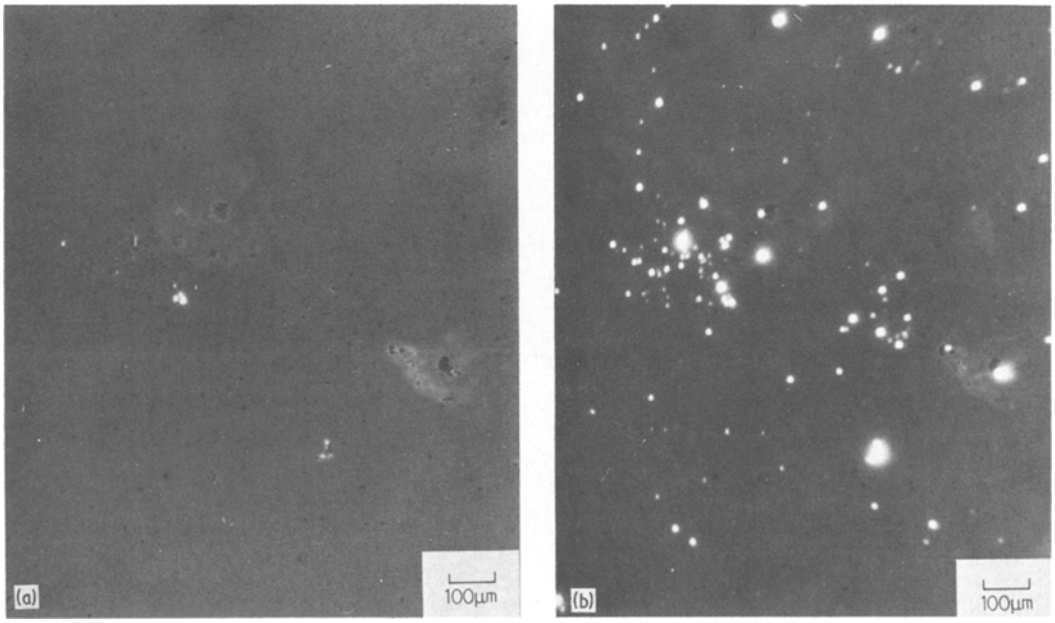

Figure 9 Polyester (M"O") film in transmitted light (a) immediately after metallization at normal incidence, (b) after light brushing to detach the dust. Dark-looking dust particles in (a) can be correlated with fresh pinholes in (b).

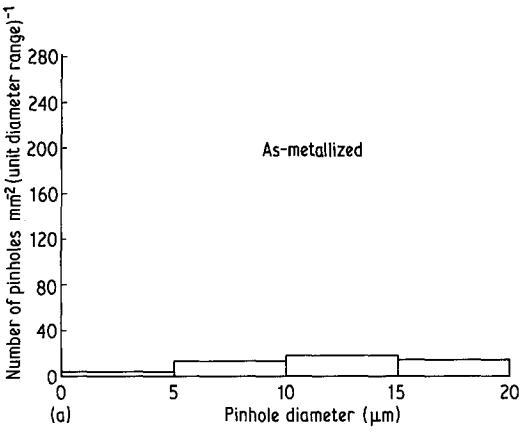

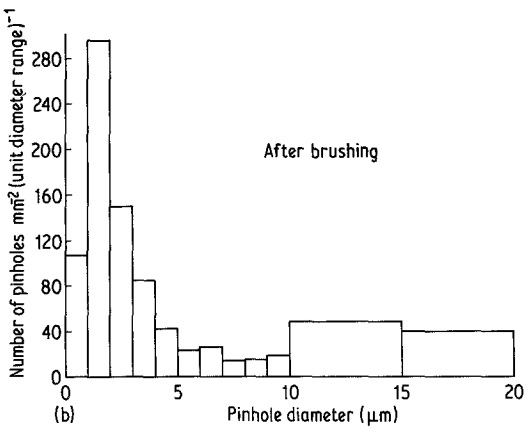

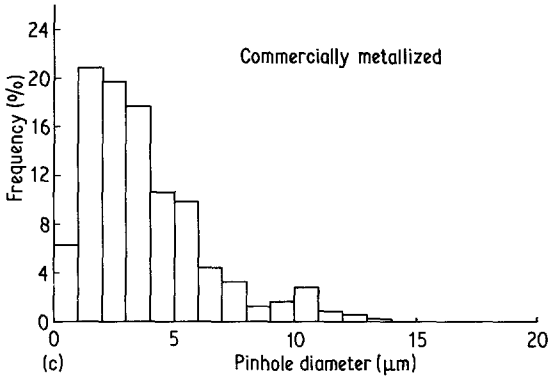

Figure 10 Distributions of pinholes according to size for: (a) Laboratory metallized (M"S") without handling; (b) as (a) but after light brushing; (c) commercially metallized polyester (M"S").

M"O" were analysed in the scanning electron microscope in an attempt to determine their origin. Fig. 13 shows the most abundant elements to be silicon, calcium and aluminium, presumably present as their oxides or salts. The intensity axis is built up on the basis of a weighting system which follows from Tables II and III, the most abundant element being assigned "4", the next most abundant "3" and so on. The filled grade, M"S", showed a very similar distribution with perhaps rather more silicon and aluminium but less calcium. However, it is not noticeably more "dusty" than M"O" film, and thus there appears no basis for considering the surface particles to be stray filler. It is significant, however, that the observed composition distribution is very typical of atmospheric dust of the size range 1 to 5 μm. Incidentally, this size of particle is notoriously difficult to remove efficiently from the air by either filtering (for which it is on the small side) or electrostatic precipitation (for which it is rather large) [17]. The most likely conclusion is that the observed surface particles result from contamination by atmospheric dust, and are unlikely to be present as a direct consequence of either the polymer film production or the metallization process.

The origin of the especially small pinholes

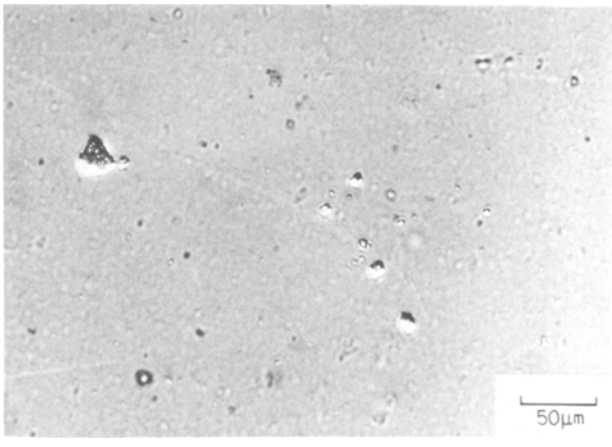

Figure 11 Polyester (M"O") film metallized at a deposition angle of 45° (from the top) showing the pinholes as shadows below the dust particles. The sample was prepared in the laboratory and not reeled (or indeed handled) in any way before examination. Transmitted light.

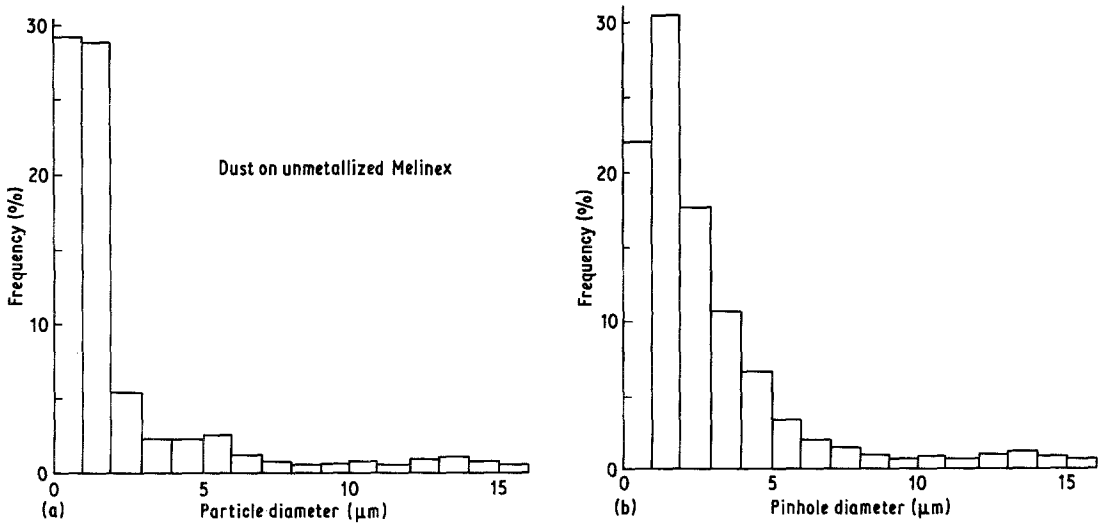

Figure 12 Comparison between size distributions of (a) particles on surface of unmetallized polyester (M"O") immediately on unreeling (counted in transmitted light), (b) pinholes in the same type of film after commercial metallization.

which could be seen very faintly in transmitted light but not at all in the TEM, has not been identified. It is possible that they may be caused by included grains of oxide, or by very narrow channels running through the film between the grains as has been seen in gold deposited on glass [18].

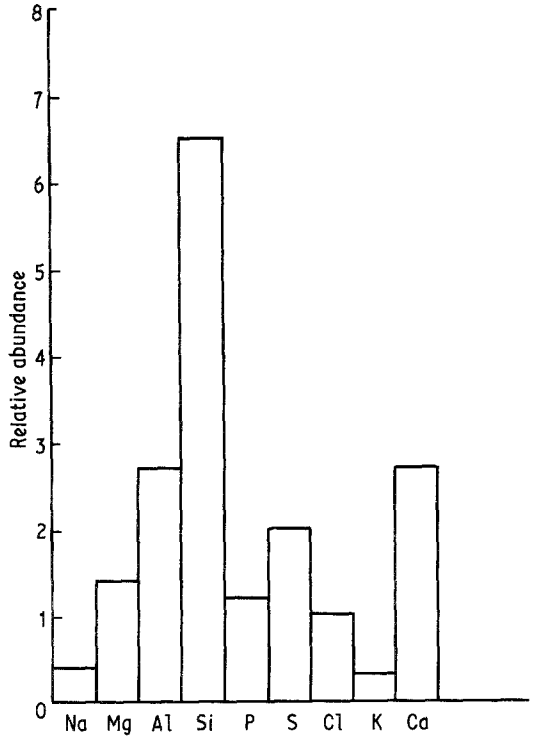

Figure 13 Distribution of detectable elements (of atomic number ≧ sodium) found in individual particles on the surface of freshly unreeled and chromium-coated film (M"O"). The elements have been weighted according to their relative concentrations. See Tables II and III. The composition of particles on filled (M"S") film was very similar.

7. Barrier properties of aluminium-coated polymer film

That a coating of aluminium 0.02 μm thick can improve the oxygen-barrier properties of 12 μm polyester film by a factor of 100 or more may seem surprising. But when one considers that aluminium is itself explosively reactive with air and that the true barrier is a few nanometres (a few lattice unit cells) of oxide, this property appears really remarkable. The oxide is an excellent barrier because of its high electrical resistivity which restricts the supply of electrons at the surface necessary for the reaction $O_2 \rightarrow 2O^{2-}$. In fact, any oxygen atom which does permeate the oxide will immediately react with the aluminium to form further oxide. So one is faced with the question as to why a coherent aluminium surface layer fails to endow the polymer with perfect barrier properties.

It follows that the actual barrier properties of the metallized film must be governed by defects in the aluminium layer. In the electron microscope the aluminium layer appears continuous except for the presence of pinholes, and it is obviously sensible to consider this type of defect to be the most likely in detracting from the perfect barrier properties. However, it is important not to lose sight of the possibility that either much finer

TABLE II Analysis of particles on Melinex 'S" film coated with chromium (on carbon stub)

Sample	Element				
	Weighting 4	Weighting 3	Weighting 2	Weighting 1	Others
1	Si	Cl	Ca	K	Sb, Fe
2	Si	P			
3	Si	Al	Fe	Ca	
4	Si	S	Al	Sb	
5	Si	Al	Sb		
6	Si	Al			
7	Si	K	S		
8	Si	Al	Ti	S	
9	Si	Ti	Cl	Al	
10	Si	Na	Cl	S	
11	Si	P			
12	Si	Cl	Al	Na	
13	Al	Ca	P		
14	Si	Al			
15	Si	Ca	Sn	Al	
16	Si	Cl	Mg	S	Al, P, K, Na
17	Si	P	Mg	S	
18	Si	Na	P		
19	Cl	K	Al		
20	Si	Al	Ca		
21	Al	P	Si	Na	Sb
22	Si	Al	Ti	Ca	
23	Si	P	Ca		
24	S	P			

defects [19] which we did not manage to observe even at × 20 000, or preferential diffusion paths perhaps along grain boundaries [20] may also contribute to the observed permeability.

8. Influence of pinholes on barrier properties

It is apparent from Fig. 14 that the measured oxygen permeability of the metallized polyester (M"S") shows some correlation with the observed pinhole density (number per mm^2). The permeability is expressed in the units of common usage, that is cm^3 oxygen/m^2/24 h, for an oxygen pressure difference of 1 atm. All the films examined for this plot were of commercial origin. The thickness of the deposited aluminium varied between specimens from 15 to 45 nm and did not appear to be related to the pinhole density. The distribution of pinhole sizes was virtually identical for the different samples, despite differences of aluminium thickness and pinhole density. It is typified by the distribution plot of Fig. 10c.

Fig. 15 shows that there is little, if any, correlation when permeability is plotted against the thickness of the aluminium layer.

The next step in determining whether the pinholes can fully account for the measured permeability is to calculate the permeability on the basis of their observed size and density. The calculation of the diffusion though a membrane from specific points (i.e. pinholes) on its surface is not especially straightforward. The amount of gas entering the polymer through a pinhole is not proportional to the area of the pinhole. This was first shown by Brown and Escombe [21] in 1900 in their classic work on the diffusion of carbon dioxide through leaf stomata, when they observed a linear dependence of diffusivity on hole diameter rather than area.

In this study we have developed a finite element approach to the calculation of diffusion from a pinhole through a polymer film. The calculations are similar to those applied to certain heat-transfer problems [22–24] although simplified in this case on account of the assumed cylindrical symmetry about the pinhole axis. The geometric framework for the calculation of permeability is shown in Fig. 16, and further details of the method are given in the Appendix. The results of calculations of permeability of 12 μm polyester (M) as a function of pinhole diameter for a fixed pinhole density are shown in Fig. 17. They are

TABLE III Analysis of particles on Melinex "O" film coated with chromium (on carbon stub)

Sample	Element				
	Weighting 4	Weighting 3	Weighting 2	Weighting 1	Others
1	Si	S			
2	Al	Mg	Si		
3	Ca	S	Si	Al	K, Fe
4	Si				
5	Ca	Al	Si		
6	Mg	Al	S		
7	Si	S			Fe
8	Si	P			
9	Si				
10	Si	Mg	Ca	Fe	Al, Ti, P
11	Fe	P	Mg	Na	Al, Si
12	Ca	Si	Fe	S	Al, Cl, K, Na
13	Si	Al	Fe		
14	Cl	S	Sb		
15	Al	Si			
16	Fe	Si	Ca		
17	Ca	Si	S	Fe	K, Na, Mg, Al, Cl
18	Fe	P	Ca	Si	K, Mn, Na
19	Si	K	Fe		Na, Mg, Cl
20	Si				
21	Cl	Na	Si	Al	
22	Si	Cl	Na	Al	
23	Si	Al	P	Cl	Fe
24	Fe	Si	Ca	Cl	Al, P, S
25	Al	Si			
26	Ca	Fe	Si	Al	S

compared with approximate calculations based on the formula for diffusion outwards from the centre of a sphere given by Barrer [25].

$$P = 4\pi D(C_1 - C_2)ab/(b - a)$$

where P is the permeability, D the diffusivity, $(C_1 - C_2)$ the concentration difference across the barrier and a and b the inner and outer radii of the spherical shell. The pinhole diameter and

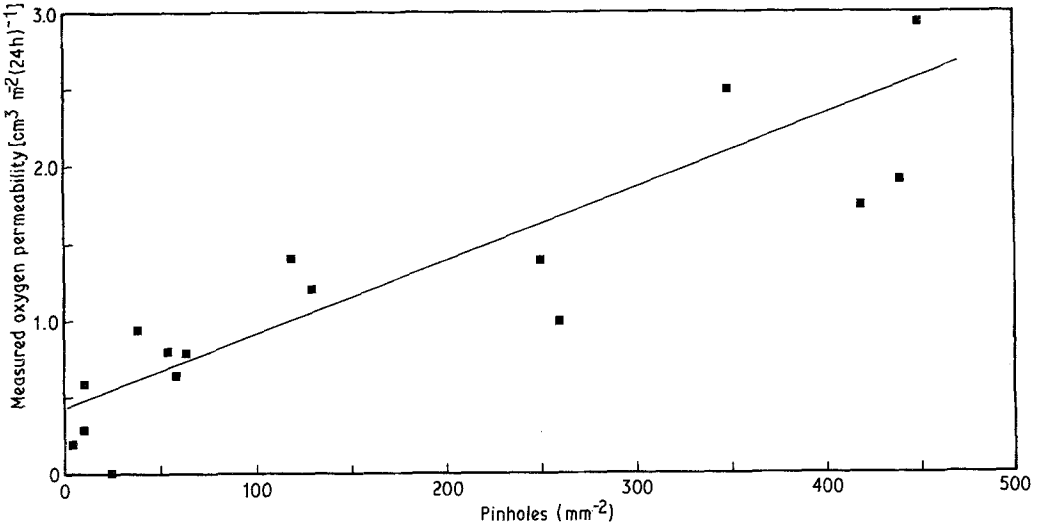

Figure 14 Plot of measured permeability for oxygen against the observed pinhole density for a range of industrially metallized samples on 12 μm polyester. The thickness of the aluminium layer varied independently of the pinhole size between 15 and 45 nm.

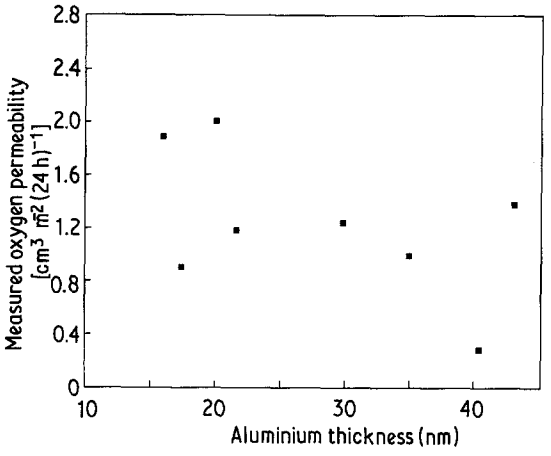

Figure 15 Plot of measured oxygen permeability against thickness of deposited aluminium for 12 μm industrially metallized polyester.

film thickness can be approximately related to *a* and *b*. The formula is only appropriate for pinholes of diameter considerably less than the polymer film thickness. Even for small pinhole diameters it tends to exaggerate the permeability, as it really assumes a hemispherical volume of polymer behind the pinhole of radius equal to the film thickness, rather than the sheet of polymer film itself. However, the approximate formula is obviously useful for the rapid estimation of permeability of metallized films where the pinhole sizes and densities are known and the diameters small compared with the film thickness.

The comparison between measured and calculated permeabilities for a range of characterized films is shown in Fig. 18. For the purposes of the calculation the pinhole diameters are taken

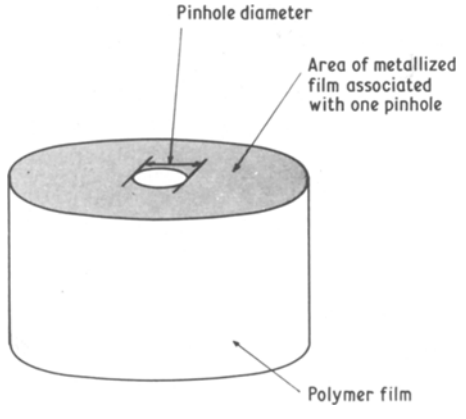

Figure 16 Diagram showing the assumption of isolated pinholes and associated cylinder of polymer used in the finite element calculation of permeability.

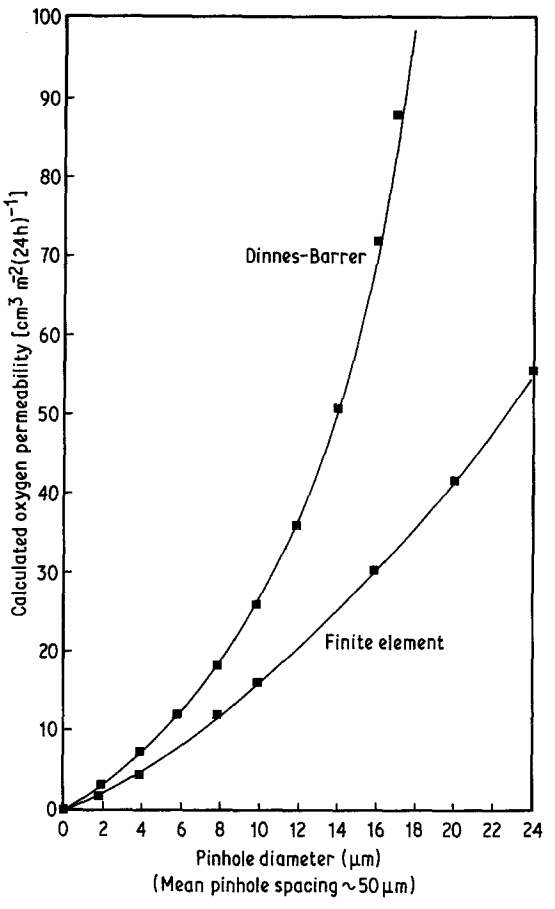

Figure 17 Permeabilities calculated as a function of a pinhole diameter. The results given by the finite element are compared with those from an approximate equation (Dinnes–Barrer).

as 2 μm which is the mean of the distribution. The existence of a quantitative correlation is very clear and confirms a basic relationship between pinhole density and barrier properties. There is some evidence of a finite intercept on the measured permeability axis, which may suggest that pinholes are not totally responsible for the observed permeability, and hence, that their complete elimination will not lead to a perfect barrier.

As a part of the finite element routine, it is possible to determine the concentration contours associated with any particular pinhole geometry. An example of such contours is shown in Fig. 19 for 12 μm polyester film and a 5 μm diameter pinhole. Perhaps not surprisingly, the concentration gradient in the polymer is especially steep just below the edge of the pinhole, and the oxygen concentration has dropped to half of its surface value within a depth of the order of one pinhole radius. The barrier properties of the polymer

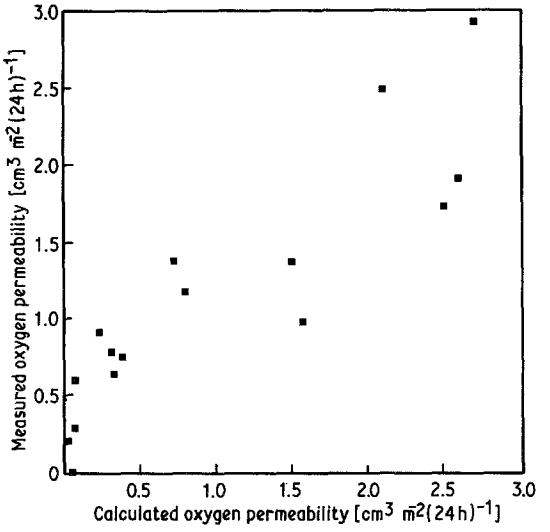

Figure 18 Plot of measured oxygen permeability against the permeability calculated on the basis of the observed pinhole size and density, for a range of commercially metallized 12 μm samples. The thickness of the deposited aluminium varies between 15 and 45 nm.

immediately below the pinhole are thus of special importance in determining the overall permeability. Another aspect of this fact is the comparative insensitivity of permeability to the polymer film thickness, especially for small pinhole sizes. This is illustrated in Fig. 20. For the typical pinhole diameter of 2 μm, the predicted barrier properties are virtually independent of polymer film thickness. One consequence of this behaviour is that if the performance of a metallized product is

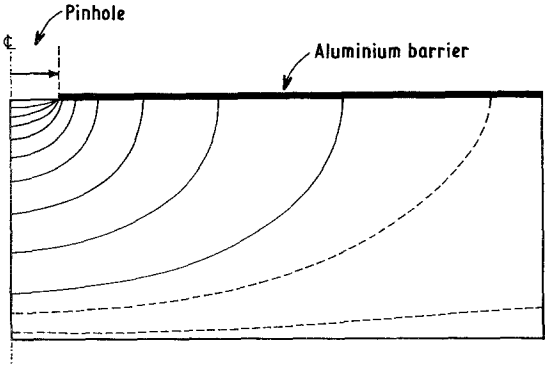

Figure 19 Calculated concentration profiles for the case of 12 μm Polyester film, with a 5 μm diameter pinhole and a mean pinhole spacing of 50 μm ($\simeq 400\,nm^{-2}$). The concentration of oxygen at the top surface at the pinhole is in equilibrium with 1 atm oxygen pressure, and that at the back surface is zero. The contours (full lines) represent equally spaced increments of concentation. Additional contours for concentrations of 0.05 and 0.025 are added as dashed lines.

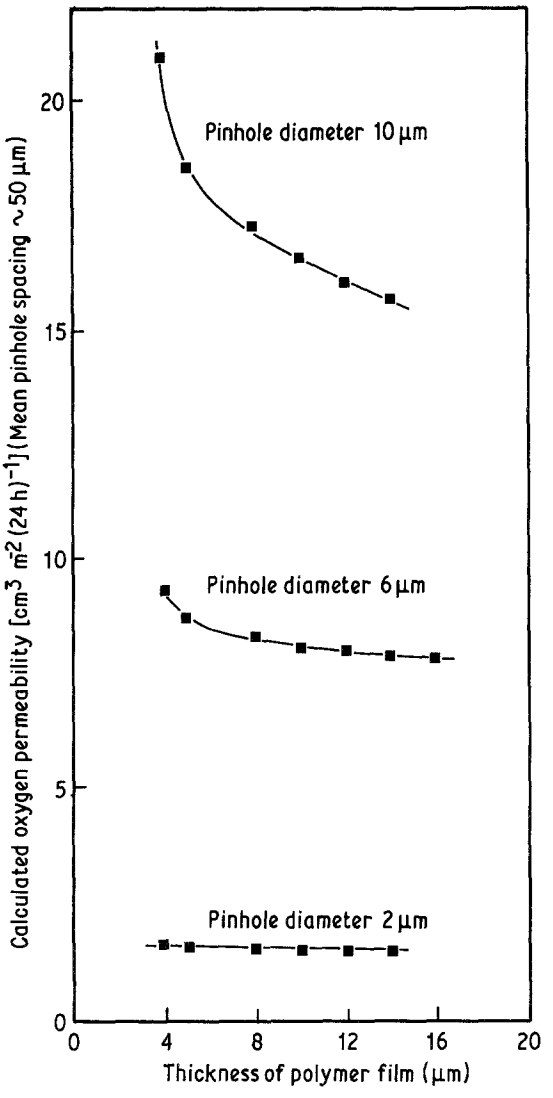

Figure 20 Plot of oxygen permeabilities calculated as a function of the thickness of the polyester film for three different values of pinhole diameter and a mean spacing of pinholes of 50 μm.

expressed in terms of an improvement ratio, that is, the ratio of permeabilities of unmetallized to metallized film, then the ratio will have meaning only for a fixed substrate thickness. It also follows that, for a given quality of metallization, the improvement ratio will be dependent on the reciprocal of the film thickness.

9. Composite polymer films

The closeness of the concentration contours just below a pinhole indicates that the permeability of the polymer in this region can have a relatively large influence on the permeability of the metallized film as a whole. Under some circumstances

the barrier properties of the surface layers of the polymer film (immediately below the metal) may be dissimilar to the bulk. For example, where the film is lacquered and then metallized over the lacquer, or where there is a polymer coating on the polymer film designed to improve barrier properties in the unmetallized condition. In these situations the effect of the metal layer (and its pinholes) on the final permeability of the film can be drastically altered. One of many composite geometries modelled by the finite element routine is shown as a concentration contour plot in Fig. 21. Here a 4 μm thick layer of material, such as lacquer, with permeability one hundred times that of the polyester, is interposed between the 12 μm polyester film and the metal layer. The contours are much more widely spaced in this layer, and for the particular case of a 5 μm diameter pinhole and a 400 nm^{-2} pinhole density, the introduction of the additional layer increases the permeability from 8 to 123 $cm^3/m^2/24$ h.

The effect of different surface layer/polyester permeability ratios on the permeability calculated as a function of pinhole diameter is shown in Fig. 22. It is the most marked for pinholes less than 5 μm diameter and shows dramatically the importance of the permeability of the surface layers of the substrate film in determining the effectiveness of an aluminium layer as a barrier.

10. Conclusions

(1) Aluminium, vacuum coated on to polyester film in thicknesses between 10 and 100 nm, is polycrystalline, the grain size being of the order of the metal thickness.

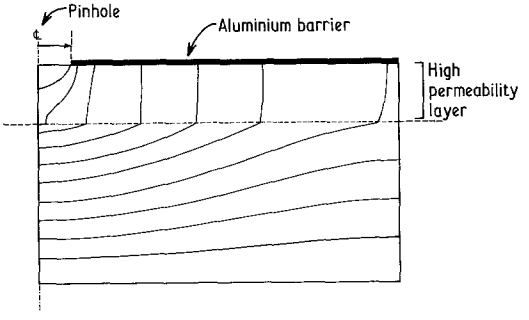

Figure 21 Calculated concentration profiles for the same set-up as in Fig. 20 (pinhole diameter 5 μm, mean spacing 50 μm, 12 μm polyester) *except* that a 4 μm thick layer of material of permeability 100 times greater than that of the polyester has been inserted between the polyester and the metal layer.

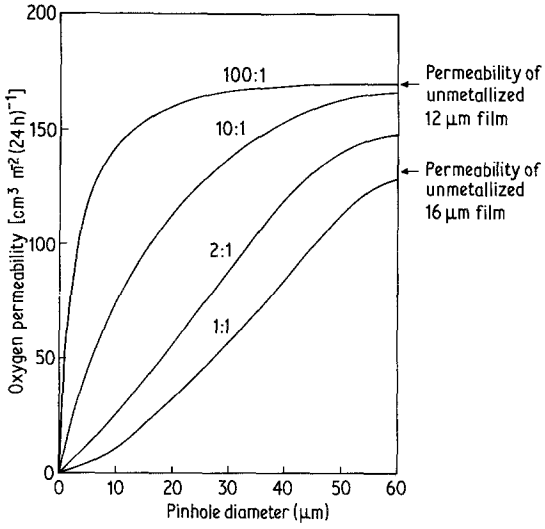

Figure 22 The effect of inserting a 4 μm layer of material with relatively poor barrier properties (greater permeability) between the metal layer and the 12 μm polyester on the permeability of the composite film. The relative permeabilities are expressed as a ratio, with that of the 4 μm layer the numerator. The plots are for a constant mean pinhole spacing of 50 μm.

(2) The grain size tends to be larger with a faster evaporation rate and/or higher vacuum.

(3) The aluminium grains show a marked texture with [1 1 1] normal to the surface of the film.

(4) Measured permeability to oxygen of the metallized films correlates linearly with the observed density of 2 to 3 μm diameter pinhole defects in the aluminium coating, but bears little, if any, relationship to coating thickness.

(5) The major cause of pinhole defects is the presence of dust particles on the polymer film surface during metallization which subsequently become dislodged and leave an unmetallized shadow. Damage by scuffing of particles can also be a source of pinhole defects which are often observed as "runs".

(6) Finite element calculations of the permeability of film coating with aluminium containing pinhole defects show: (a) that the oxygen permeability calculated for pinhole density observed for a particular sample agrees with the permeability measured on that sample; (b) for pinholes of diameter 2 μm or less, the permeability of a metallized film is virtually independent of the thickness of the polymer substrate; (c) the barrier properties of the surface layers of the polymer film immediately beneath the metal coating are

critical in determining the permeability of the metallized film.

Acknowledgements

The authors wish to thank Dr D. J. Blundell of ICI (Plastics and Petrochemicals) and Mr R. Collins for their association with the work, Professor R. W. K. Honeycombe for the provision of facilities, and S.E.R.C. and ICI Ltd, for funding in the form of a CASE studentship.

Appendix

The basis of the finite element model is a two-dimensional net of points, representing a cylinder of the laminate, as in Fig. 16.

At each point the equation:

$$w_1 C_1 + w_2 C_2 + w_3 C_3 + w_4 C_4 = (w_1 + w_2 + w_3 + w_4) C_0$$

is applied (where $C_0, \ldots, C_4$ represent oxygen concentrations, C_0 being at the point under considerations, and $w_1, \ldots, w_4$ are weightings that allow for two-dimensional representation of a three-dimensional problem). This creates a new array of points, and the equation is repeatedly applied until the system converges.

The concentration of oxygen on the pinhole side is taken to be atmospheric (normalized to 1.0) whereas on the far boundary it is taken as zero. The outer boundary has a reflection condition imposed which in effect prevents oxygen crossing it, similarly along the pinhole axis and the metal/polymer boundary.

The choice of initial array in such relaxation techniques is significant in terms of the number of iterations required. For a system composed of one material the points are readily set up. The pinhole axis is assumed to show a constant gradient from 1.0 to 0.0, the metal/polymer boundary is set up as a logarithmic decay from 1.0 to some assumed value at the outer surface of the cylinder. All remaining points within the net are set up using linear decay from metal to vacuum.

In the situation where there is a laminate of two materials of different diffusivity, then the problem is more complex. It is necessary to find a method that will maintain different concentration gradients in each material. This was initiated at the interface where the weightings in the vertical direction are different in the ratio of diffusivities for the two component materials.

The permeability is calculated using a method based on comparison with unmetallized film (the permeability of uncoated 12 μm polyester (M) is known to be 170 $cm^3/m^2/24$ h) and thus the concentration of oxygen at any point within a sheet of polymer may be calculated. The ratio of

(a) the oxygen concentration gradient between (i) a plane, parallel and adjacent to the lower (vacuum) boundary and (ii) the lower (vacuum) boundary itself, with

(b) the oxygen concentration gradient across an equivalent plane in uncoated 12 μm polyester (M)

is taken as the ratio of the permeabilities of the metallized and unmetallized films.

A standard pinhole spacing of 5 μm was used for most calculations (equivalent to 4×10^8 pinholes/m^2). A uniform pinhole diameter was assumed, and any overlap taken to have a negligible effect [16]. The diffusion volume associated with each pinhole was taken as a cylinder, the circular cross-section of which was equal to the reciprocal of the pinhole density.

References

1. S. KUT, *Metal Finishing* 43 (1975) 568.
2. S. KUT, in "Science and Technology of Surface Coating", edited by B. N. Chapman and J. C. Anderson (Academic Press, New York, 1974) p. 43.
3. S. KUT, *Prod. Finish.* 38(7) (1974) 45.
4. *Idem, ibid,* 38(9) (1974) 89.
5. L. P. ANDERSON and B. C. KEMP, Metallised Packaging Films in the US Market, 3rd ICI European Metallising Symposium, Venice (1978).
6. S. R. VELJKOVIC and P. BIBOVIC, *Vacuum* 27 (1978) 141.
7. D. W. PASHLEY, *Adv. Phys.* 14 (1965) 361.
8. J. FRIDRICH and K. KOHOUT, *Thin Solid Films* 7 (1971) 49.
9. W. B. PENNEBAKER, IBM Research Report, RC2015 (1968).
10. P. J. CHAUDHARI, *Vac. Sci. Technol.* 5(9) (1966) 520.
11. M. LAUGIER, *Thin Solid Films* 79 (1981) 15.
12. J. C. BLAIR and P. B. GHATE, *ibid.* 72 (1980) 449.
13. S. TOLENSKI, "Multiple Beam Interferometry" (Clarendon Press, Oxford, 1948).
14. E. H. H. JAMIESON, PhD thesis, Cambridge (1980).
15. H. P. KLUG and L. E. ALEXANDER, "X-Ray Diffraction Procedures for the Polycrystalline and Amorphous Materials", 2nd edn (Chapman and Hall, London, 1974).
16. B. J. MULDER, *Vacuum* 28 (1978) 11.
17. R. CLIFT, private communication (1979).
18. J. R. LLOYD and S. NAKAHARA, *Thin Solid Films* 45 (1977) 411.

19. I. A. BLECH and E. S. MEIERAN, *J. Apply. Phys.* **40** (1969) 485.
20. M. M. GUDIMOV, *Fiz. Khim. Mekh. Mater.* 7(2) (1971) 59.
21. H. BROWN and F. ESCOMBE, *Phil. Trans. Roy. Soc. Lond.* **B193** (1900) 223.
22. G. E. MYERS, "Analytical Methods in Conduction Heat Transfer" (McGraw-Hill, New York, 1971).
23. D. N. deG. ALLEN and S. C. R. DENNIS, *J. Mech. Appl. Maths.* **4**(2) (1951) 2.
24. J. R. WHITEMAN, *ibid.* **21** (1973) 41; *ibid.* **23** (1973) 449.
25. R. M. BARRER, "Diffusion In and Through Solids" (Cambridge University Press, 1951).

Received 11 May
and accepted 26 May 1982